Astron. & Astrophys. 24, 283–293 (1973)

On the Stability of the Planetary System

J. Birn
Institut für Astrophysik
Technische Universität Berlin

Received December 20, 1972

Summary. Numerical experiments of the n-body type have been carried out to test the stability of the planetary system. The orbits of the planets have been followed by means of numerical integration, starting with various initial configurations. It has been found that stable orbits occur only within certain stability zones, in the central part of which the present orbits lie. The stability limits coincide with commensurabilities of the type $(n+1):n$. The results are confirmed by analytical discussion by means of the jacobian integral. The stability limits of orbits of planetoids are also discussed.

Key words: planetary distances – evolution – commensurabilities

1. Introduction

The regularity of planetary distances from the sun, described by the well known Titius-Bode law

$$r_n = 0.4 + 0.3 \cdot 2^n \text{ (in AU, } n = -\infty, 0, 1, \ldots, 8) \qquad (1)$$

is not fully explained yet. Does it have any simple physical meaning? There are two possible physical processes, which could have caused this regularity:
1) The distribution of planetary matter in form of gas and dust determined the distribution of the planets before their final condensation. Such a distribution would primarily be produced by gaskinetic processes.
2) The distances of the planets changed after their condensation, until they relaxed in the present configuration through interactions. (This includes the possibility that the system started with more than 9 planets, of which the rest was thrown out by interaction.) In this case the distribution would be the product of gravitational interaction (n-body problem).
In either case, if the present configuration is produced by the first or the second alternative it was influenced in the past by perturbations. Therefore, we have to investigate the limits of stability. As is well known, the present configuration is stable over long time scales ($\sim 10^7$ yrs, e.g. Williams and Benson, 1971).
Stability of orbits has been treated analytically in the framework of the restricted three-body problem (e.g. Szebehely, 1967; Giacaglia, 1970). Stabilities of stellar clusters, i.e. systems of a great number of masspoints have been examined by use of numerical integration of orbits (e.g. Hoerner, 1960, 1963). Discussions about the stability of the planetary system (for references, see Hagihara, 1961) are still unsatisfactory. Ovenden (1972) studied the stability of the planetary system by means of the "principle of least interaction action", which yields the present planetary distances under the assumption that an additional planetary mass ($\sim 90\, m_\oplus$) was present between Mars and Jupiter until 16 million yrs. ago. Hills (1971) followed the evolution of various systems of planets by means of numerical integration of orbits. He found the period of neighbouring planets often to be commensurable with ratios lying between $9/4 = 2.25$ and $8/3 = 2.67$. From this follows that the periods and subsequently the semi-major axes obey approximately a geometric series, which is often used instead of (1) (Weizsäcker, 1943, ter Haar and Cameron, 1963). The stability of these systems was not discussed in detail. Furthermore, his study was restricted to a few configurations partly chosen at random.
In the present paper we shall study, by means of numerical integration of orbits, the evolution of an ensemble of configurations, which for the sake of generality is as complete as possible. Those configurations in which the semi-major axes of all orbits remain constant over long time scales (except for oscillations) are regarded as stable. The method employed also allows to obtain information on stable orbits of planetoids and other possible (hypothetic) planets.

2. Initial Conditions

In order to make, different configurations compatible, we postulate that energy and angular momentum is the same for all initial configurations. Even with this

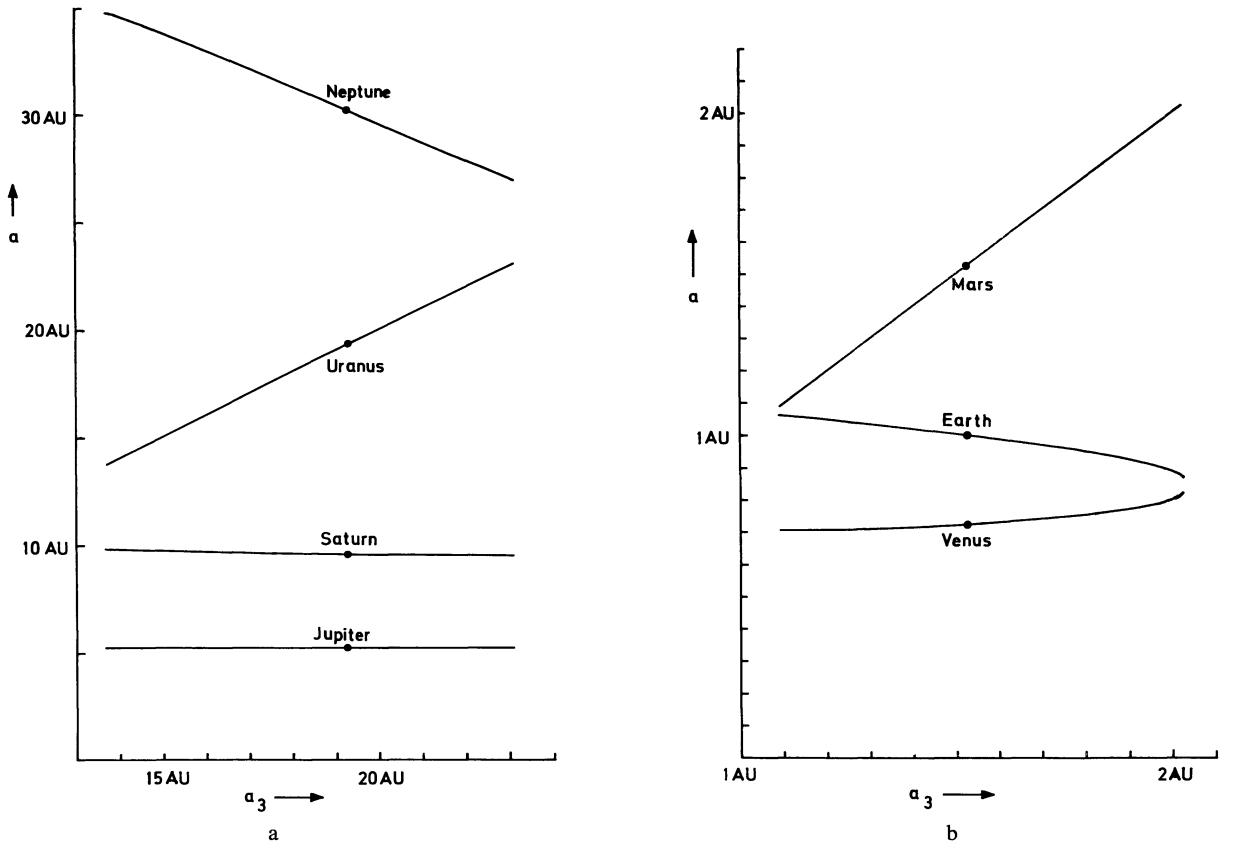

Figs. 1a and b. Initial semi-major axes, a of the outer planets (Fig. 1a) and the inner ones (Fig. 1b) versus initial semi-major axis of the third planet, a_3 (Uranus in Fig. 1a, Mars in Fig. 1b). The semi-major axes of a special configuration are connected by a vertical line. The dots mark the present distances

restriction there remain $6n$-4 free parameters that determine an initial configuration of n planets. To reduce the number of parameters further, additional assumptions are made:

1) The system has been subdivided into two groups:
(a) the major planets Jupiter, Saturn, Uranus, and Neptune (the other planets have a negligible influence on these four on account of their comparatively small masses and can be omitted)
(b) the inner planets Venus, Earth, and Mars as well as Jupiter (the influence of the other major planets is small in comparison to Jupiter; Mercury can be omitted on account of its small mass).
The total energy and angular momentum were fixed in group (a) as well as in group (b).
The planetoids (including Mercury) have been treated as test bodies of negligible masses in the present system of Venus, Earth, Mars, and Jupiter.
2) The initial distance of Jupiter has been fixed for reasons of normalization.
3) The inclinations are assumed to be zero.
4) The initial eccentricities have been set to zero in order to find a maximum number of stable orbits (configurations with smaller eccentricities are generally more stable than those with larger ones) and because the actual eccentricities are small.
5) The initial longitudes of the planets have been arbitrarily chosen (the choice of these longitudes has usually no influence on the stability of the system, except for special commensurable orbits).

With these assumptions, there is only left one free parameter to determine an initial configuration. If for example in (a) the distance of Uranus is chosen, the distances of Saturn and Neptune are determined.
Figure 1 shows the allowed initial distances of the planets for the two groups (a) and (b), plotted versus the distances of Uranus (a) and Mars (b), respectively. In the case of (b) the (constant) distance of Jupiter is not shown. The masses of the planets have been raised in order to reduce computational effort (see also Section 8). The mass factor is 20 in case (a), and 10 for Jupiter and 100 for the rest in case (b).

3. Differential Equations and Orbit Integration

The most appropriate method to calculate stable orbits is the integration of the elements. The computational effort per integration step is on one hand large in comparison with the integration of the cartesian coordinates; on the other hand, the method allows larger integration steps because the elements are nearly

constant. This results in a greater stability against round-off and truncation errors and consequently in greater accuracy. Differential equations are obtained by the method of variation of elements (e.g. Stumpff, 1965). In order to avoid singularities because of zero inclination and small eccentricity, we employ instead of the usual elements $-a$ (semi-major axis), e (eccentricity), i (inclination, here $= 0$) ω (argument of the perihelion), Ω (longitude of the ascending node) and t_0 (epoch) –, the four coordinates

a,

$\xi = e\cos\tilde{\omega}$

$\eta = e\sin\tilde{\omega}$

$\lambda = M + \tilde{\omega}$

($\tilde{\omega} := \Omega + \omega$ is the longitude of the perihelion, M is the mean anomaly, λ is the mean orbital longitude)
With $\boldsymbol{K}_i$, the perturbation force acting on the i-th planet,

$$\boldsymbol{K}_i = -k^2 \sum_{\substack{j=1 \\ j\neq i}}^{N} m_j \left(\frac{\boldsymbol{r}_i - \boldsymbol{r}_j}{|\boldsymbol{r}_i - \boldsymbol{r}_j|^3} + \frac{\boldsymbol{r}_j}{|\boldsymbol{r}_j|^3} \right) \quad (i = 1, \ldots, N)$$

(r_i is the heliocentric distance of the i-th planet) the four differential equations for a, ξ, η, and λ (after Kristensen, 1970, with zero inclination):

$$\begin{aligned}
\frac{da}{dt} &= 2\frac{(\boldsymbol{v}\boldsymbol{K})}{n^2 a} \\
\frac{d\xi}{dt} &= \frac{\sqrt{1-e^2}}{na} K_y - \frac{(\boldsymbol{r}\boldsymbol{v})}{n^2 a^3} K_x + \frac{x(\boldsymbol{v}\boldsymbol{K})}{n^2 a^3} \\
\frac{d\eta}{dt} &= -\frac{\sqrt{1-e^2}}{na} K_x - \frac{(\boldsymbol{r}\boldsymbol{v})}{n^2 a^3} K_y + \frac{y(\boldsymbol{v}\boldsymbol{K})}{n^2 a^3} \\
\frac{d\lambda}{dt} &= n - 2\frac{(\boldsymbol{r}\boldsymbol{K})}{na^2} + \frac{1}{1+\sqrt{1-e^2}} \left(\xi \frac{d\eta}{dt} - \eta \frac{d\xi}{dt} \right)
\end{aligned} \tag{2}$$

$\boldsymbol{v}$ is the velocity of the planet in question, (x, y) and (K_x, K_y) are the coordinates of $\boldsymbol{r}$ and $\boldsymbol{K}$ in the coordinate system adopted. The indices which number the planets are omitted.
The system (2) was integrated by a 6-th order Runge-Kutta method, given by Mikhlin and Smolitsky (1967). The time steps were variable and were adjusted to the momentary perturbation force.
The adopted method is appropriate to elliptical or quasi-elliptical orbits; it fails when the eccentricity becomes $\geqq 1$, that means, when the orbit (or a part of it) becomes parabolic or hyperbolic. Such highly eccentric orbits should become unstable. The integration of the orbit was stopped at this point.
An example of an unstable system is shown in Fig. 2, in which the distances of the four major planets from the sun are plotted as a function of time. The distances

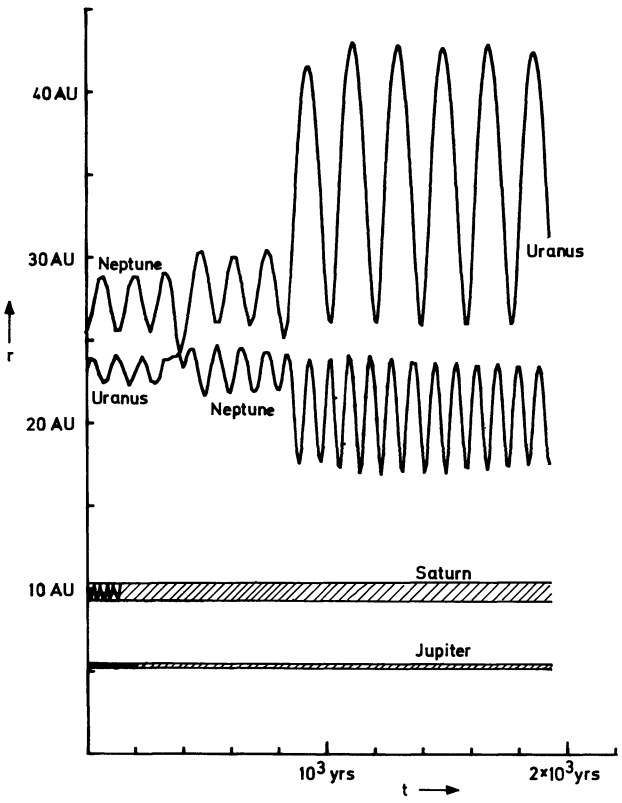

Fig. 2. Evolution of an unstable configuration. The distances of the four major planets are plotted as function of time

of Jupiter and Saturn only oscillate and are indicated by their aphelion and perihelion distances (hatched strips). There are obviously two close encounters of Uranus and Neptune. The first one causes an interchange of the two planets, the second one leads to a strong increase of the eccentricities coupled with an enhanced separation of the mean distances.
To test the accuracy of the orbits, the total energy E and the angular momentum J have been computed during the experiments. The relative errors at the end of an experiment amounted to $3-5\cdot10^{-9}$ for E and J in case (a), and $2-4\cdot10^{-7}$ for E and $2-3\cdot10^{-8}$ for J in case (b). The coordinates of especially the lower mass planets are more sensitive than E and J to round-off and truncation errors. Therefore some orbits have been recomputed by using half the stepsize. The result was that at the end of the integration the (especially sensitive) angular coordinates (lying between 0 and 2π) remained accurate at least within 3 decimals, while the major axes remained accurate at least within 6 decimals.
The integrations covered in case (a) a period of approximately 2000 yrs, in some instances up to 10000 yrs, and in case (b) 700 yrs, in some instances 1500 yrs. The time scales, in which instabilities occurred, are of the order of 500 yrs (case (a)) and 10 to 30 yrs (case (b)).

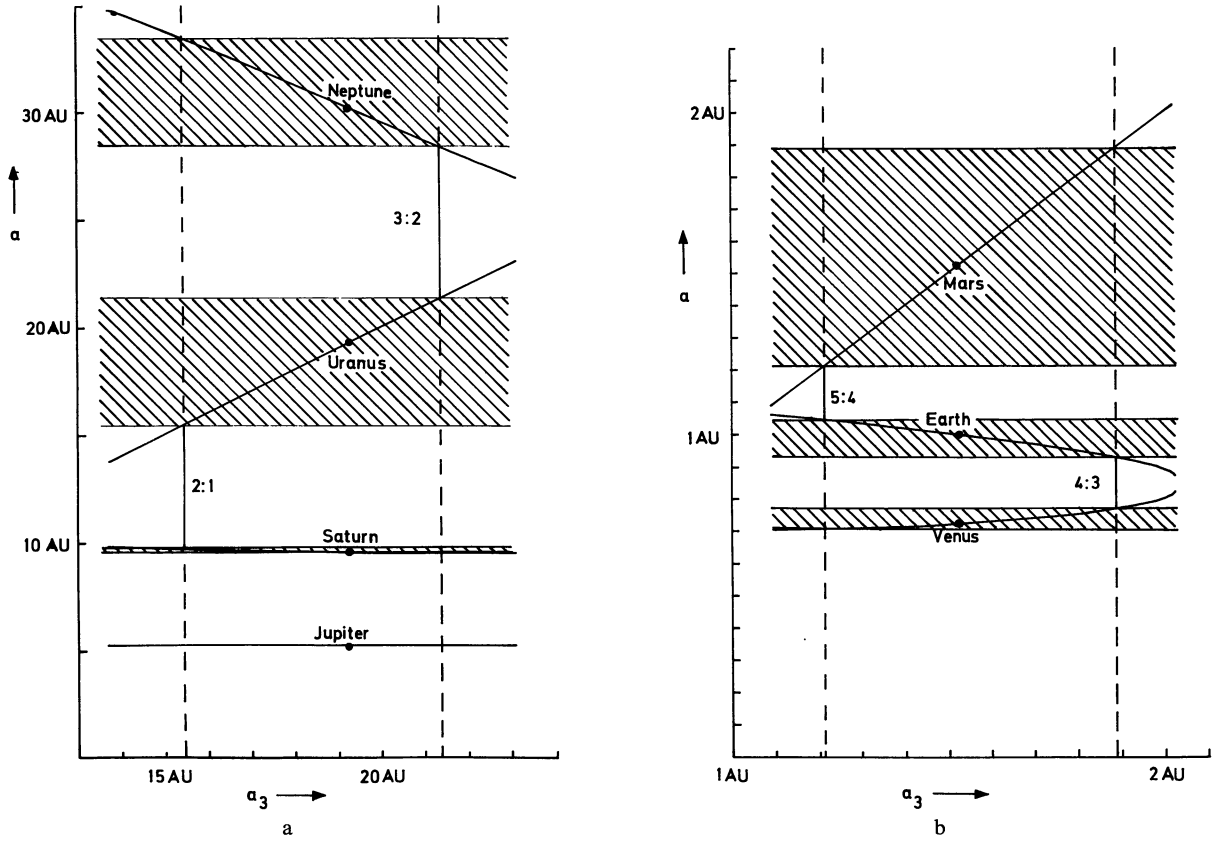

Figs. 3a and b. Stability zones of the semi-major axes of the outer planets (Fig. 3a) and the inner ones (Fig. 3b). The numbers indicate the limiting commensurabilities

4. Results

In Fig. 3 the semi-major axes of the initial configurations are plotted again as in Fig. 1. In addition, the limits which are found for stable configurations are indicated by vertical dashed lines. The resulting semi-major axes of stable systems lie in the hatched areas. The limits of stability coincide with simple commensurabilities of the periods of two neighbouring planets, i.e. 2:1 for Uranus and Saturn and 3:2 for Neptune and Uranus (case (a)), and 4:3 for Venus and Earth and 5:4 for Mars and Earth (case (b)). The commensurabilities are of the type $(n+1):n$.

Instructive is the evolution of configurations in vicinity of one of these limiting commensurabilities as well as near other simple commensurabilities within the stability limits. In Fig. 4 the ratio of the periods of two neighbouring planets (averaged over 0 to t) is plotted as a function of time. The dashed lines mark commensurabilities of the type $(n+1):n$. If the ratio of the initial periods is clearly smaller than the limiting commensurability, the configuration becomes unstable. However, if it is slightly below the limit, the orbits change in such a way that the period ratio, averaged over long times (about 500 yrs in case (a), and about 20 yrs in case (b)), exceed slightly the limiting commensurability. The same behavior becomes also evident at some other critical commensurabilities which are closest to the limit inside the stability zone (Figs. 4c and d). If the ratio of the periods is initially larger than such a commensurability, both at the limit and above, it remains practically constant.

As a consequence of this behavior, the stability zones of the mean semi-major axes are smaller than those of the initial distances. Another consequence is those gaps appear in the stability zones at the critical commensurabilities, similar to the Kirkwood gaps in the asteroid belt. However, in contrast to these, the gaps which we have found appear only at commensurabilities of the type $(n+1):n$.

An exception of the rule described above is shown in Fig. 4a. Here we find stable configurations below the limiting commensurability 2:1 within a narrow band. The lower limit of this band does not coincide with a commensurabilities of type $(n+1):n$, but of type $(n+2):n$ (5/3). It is not clear, if the stability of these configurations is only simulated by a relatively high lifetime. But the persistantly small eccentricities point to stability.

5. Orbits of Planetoids

The present configuration of Venus, Earth, Mars, and Jupiter was chosen as initial configuration (with the re-

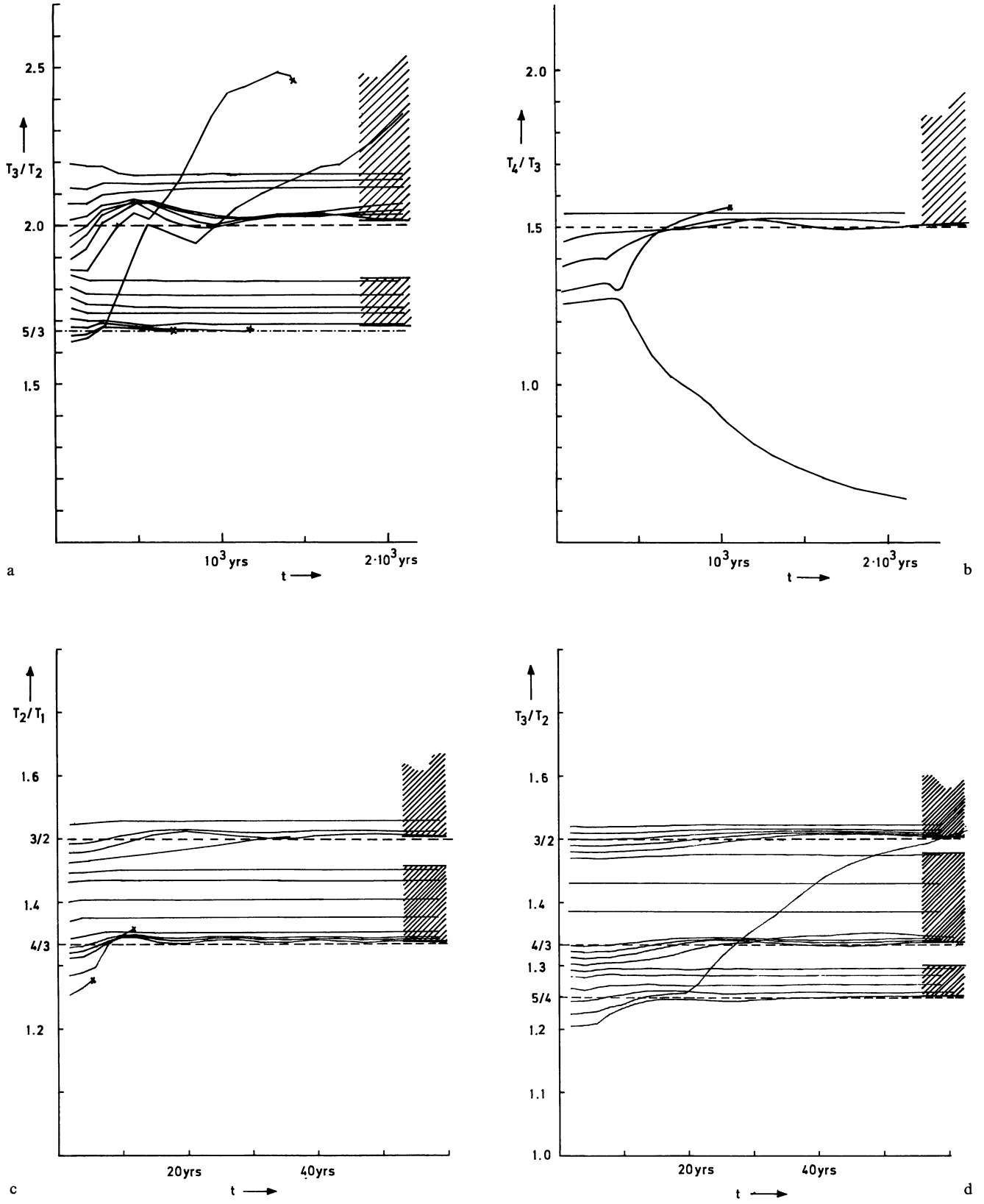

Figs. 4a–d. Evolution of the period ratios (averaged from 0 to t) of Uranus and Saturn (Fig. 4a), Neptune and Uranus (Fig. 4b), Earth and Venus (Fig. 4c), and Mars and Earth (Fig. 4d) for a number of configurations. The hatched areas indicate the stability zones. Crosses mark the end of integration (when $e \geqq 1$)

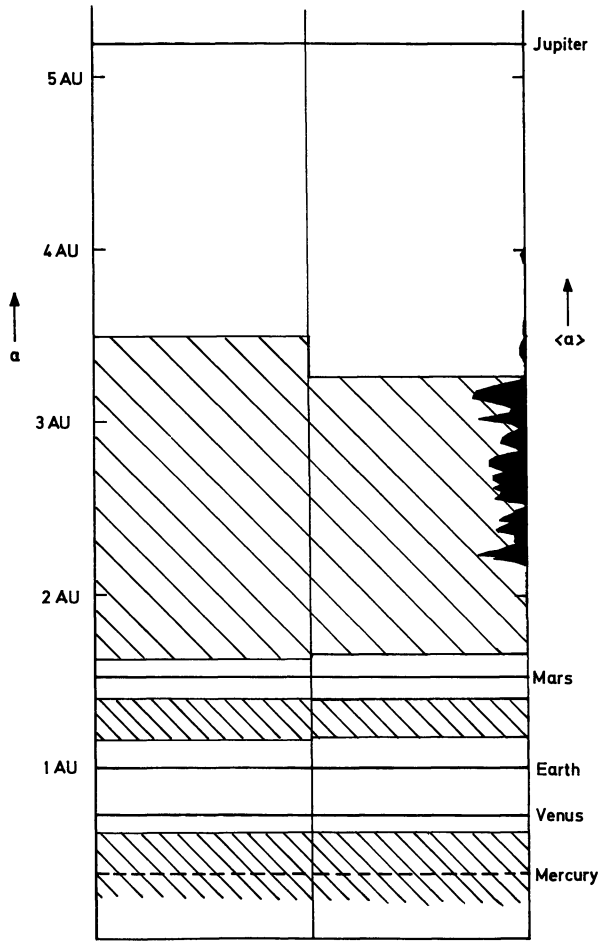

Fig. 5. Stability zones of the semi-major axes of planetoids (hatched areas). Left side: initial distances of stable configurations. Right side: mean semi-major axes. Mercury is treated as a planetoid. Its distance lies in the stability zone (dashed line). The observed frequency distribution of planetoids is indicated on the right hand side

strictions of Section 2). The planetoids were placed as massless test bodies at various distances between 0.64 AU and 5.2 AU. Their initial eccentricities as well as those of the planets were assumed to be zero. Figure 5 shows the stable zones of semi-major axes of the planetoidal orbits (hatched areas). In Figs. 6a–c the evolution of the periods of the planetoids (as ratio to the period of the nearest planet) is shown (averaged from 0 to t). The periods of stable orbits lie either outside a zone around the period of the relevant planet, which is limited by commensurabilities of the type $(n \pm 1):n$, or exactly at the ratio 1. The latter yields the well known librations around the lagrangian triangular points, which are realized by the Trojans. No stable orbits appear between Venus and Earth. Most obvious is the limiting commensurability 1:2 with respect to the Jupiter period. This fits well into the observed increase of the frequency of asteroids with periods below this critical value. It should also be mentioned that runs with a hundredfold Jupiter mass yield a stability limit at 1/3 of the Jupiter period.

Some of the results of the present paper can be compared with results of Kumar and Shelus (Shelus and Kumar, 1970; Kumar, 1971), who treated periodic orbits in the restricted three-body problem. Some of the orbits, they found unstable, lie within our stability limits. However, the detailed discussions of the previous and the present section have shown, that those periodic orbits (i.e. orbits with periods commensurable to that of Jupiter) fall into the small gaps at the critical commensurabilities within the stability zones. This means that the study of periodic orbits preferably selects unstable cases. Accordingly, the instability of orbits obtained with an increased Jupiter mass does not allow the conclusion that the primeval mass of (proto-) Jupiter did not exceed the present value (Kumar, 1971).

6. Analytical Discussion of the Results

The experiments have shown that simple commensurabilities of two neighbouring planets limit the stability zones. This means that the interaction of these two planets is responsible for the limits. Therefore, it should be possible to deduce these limits from the three-body problem (the sun + two planets). The simplest case is the restricted three-body problem, which can best be applied to the system Sun, Jupiter, and planetoid. For this reason we treat this problem first.

6.1 Planetoids

In the n-body problem a system is characterized by total energy and angular momentum. In the restricted three-body problem, the respective conservation law is the jacobian integral

$$2U - \left(\frac{\partial \boldsymbol{r}}{\partial t}\right)^2 = \mathrm{C} = \mathrm{const} \tag{3}$$

where

$$U = k^2\left(\frac{m_\odot}{|\boldsymbol{r}-\boldsymbol{r}_\odot|} + \frac{m_\mathrm{J}}{|\boldsymbol{r}-\boldsymbol{r}_\mathrm{J}|}\right) + \frac{1}{2}(\boldsymbol{d}\times\boldsymbol{r})^2$$

is a potential function depending only on $\boldsymbol{r}$.

$\boldsymbol{r}$, $\boldsymbol{r}_\odot$, $\boldsymbol{r}_\mathrm{J}$ are the center-of-gravity coordinates of the planetoid, the sun, and Jupiter; $m_\odot$, m_J are the masses of the sun and Jupiter; $\boldsymbol{d}$ is a vector perpendicular to the orbital plane of Jupiter with an absolute value equal to the mean motion of Jupiter; k is the gaussian constant; and $\partial\boldsymbol{r}/\partial t$ is the velocity of the planetoid in the co-rotating system.

The jacobian constant C is fixed by the initial conditions. With this, the absolute value of the velocity in

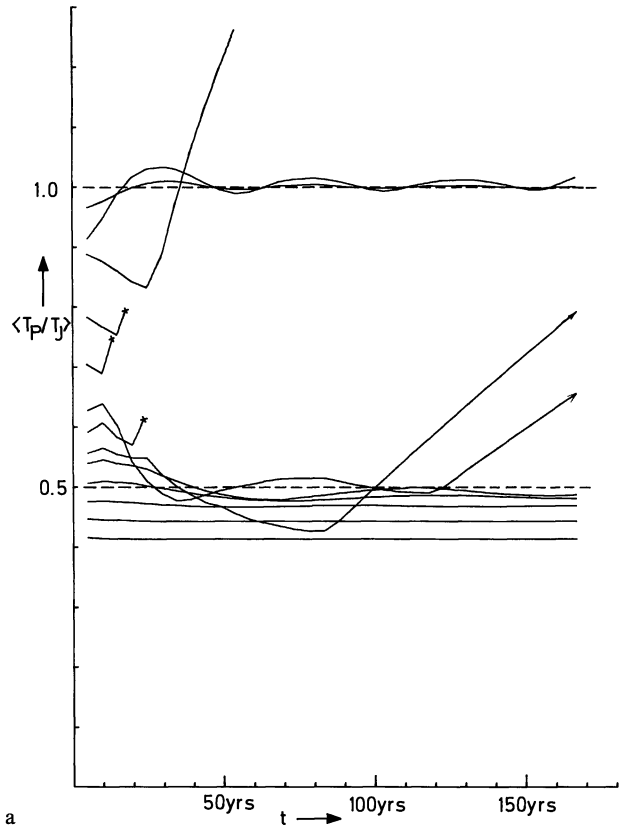

a

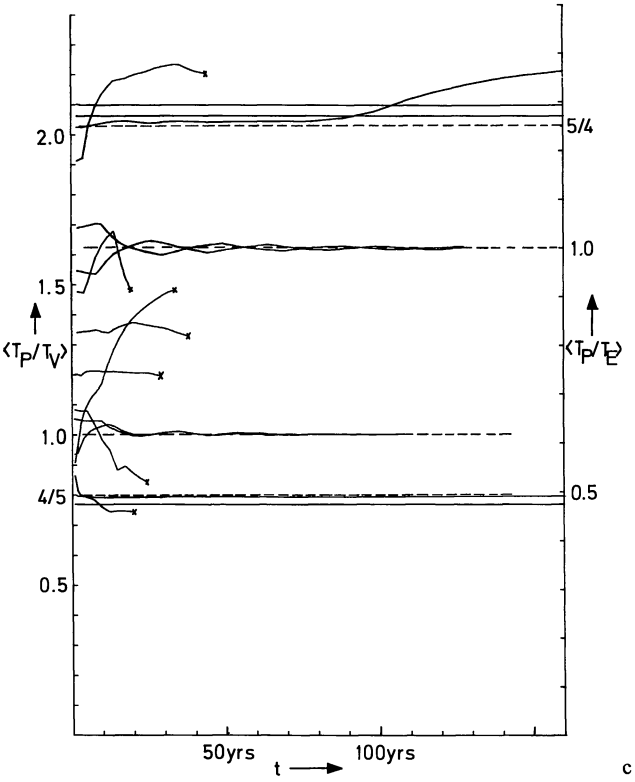

c

Figs. 6a–c. Evolution of the period of planetoids, T_P (averaged from 0 to t). The ordinate gives the ratio of the period to that of Jupiter (T_J), Mars (T_M), Earth (T_E), and Venus (T_V). Dashed lines indicate commensurabilities of the type $(n+1):n$ and the ratio 1. Crosses mark the end of integration (when $e \geqq 1$)

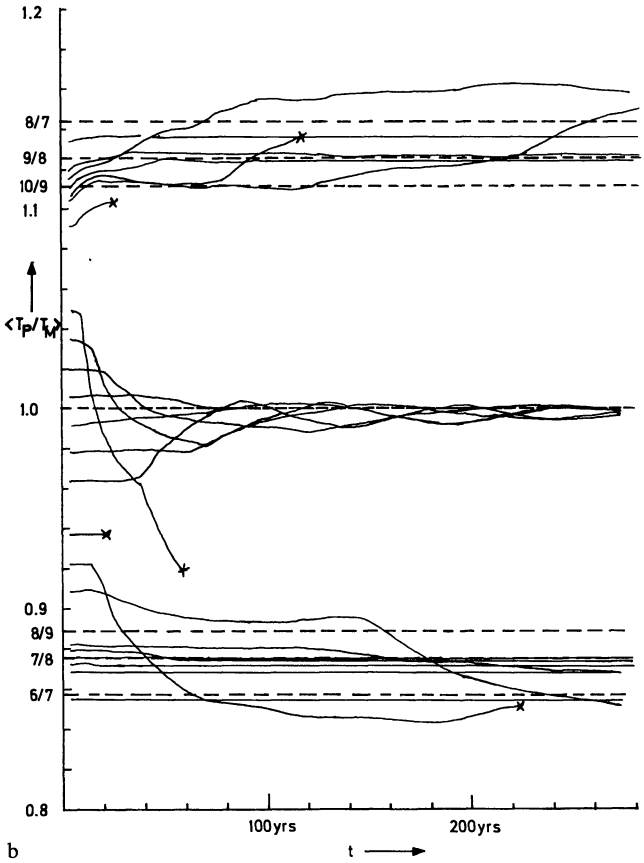

b

the co-rotating system is determined at every point of the plane by Eq. (3) $(\partial \boldsymbol{r}/\partial t)^2 = 2U - C$.

In the regions, where we have $2U - C < 0$, no real solution of the velocity exists. These regions can never be reached by a planetoid with the chosen initial conditions. The boundary of the accessible area is then given by the "zero-velocity curve"

$$2U(\boldsymbol{r}) - C = 0\,, \tag{4}$$

along which the velocity of a planetoid is zero in the co-rotating frame of reference.

In Fig. 7 typical forms of zero-velocity curves are demonstrated for various values of C. The hatched areas are the forbidden ones ($2U - C < 0$). For large values of C (larger than a certain C_1) the zero-velocity curve consists of three separate, almost circular, curves (Fig. 7a). Here the two inner regions around Sun and Jupiter are allowed as well as the region outside the large oval. Transition from one region to another is not possible. A planetoid, whose orbit around the sun lies inside the Jupiter orbit, can therefore never leave this area. For smaller values of C, the inner regions merge (Fig. 7c, d). For $C = C_1$ (Fig. 7b), the inner part of the zero-velocity curve is identical with the known Roche limit. For still smaller values of C ($C < C_2$), the inner

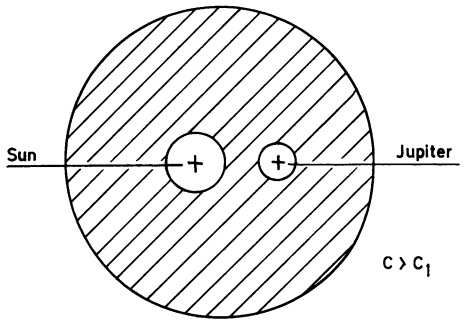

a

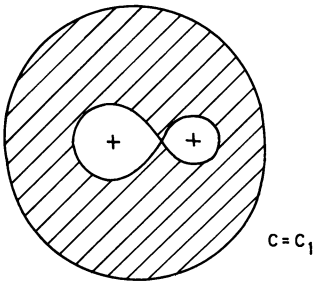

b

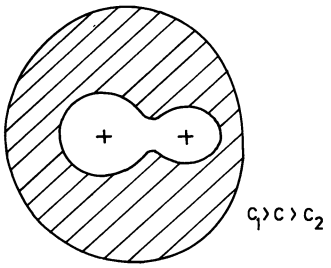

c

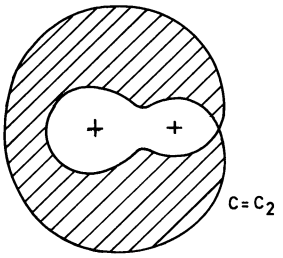

d

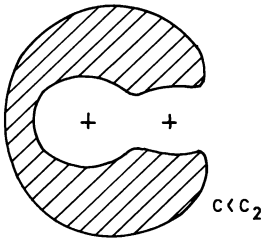

e

Figs. 7a–e. Typical forms of zero-velocity curves in a co-rotating frame for several values of C

region connects with the outer region (Figs. 7d, e). In these cases, unstable orbits are possible, along which a planetoid will leave the inner (Jupiter) region. In a configuration with $C > C_1$, the orbit of a planetoid within the inner region around the sun, should be definitely stable. So one is able to predict the stability of the planetoidal orbit from the initial conditions by the calculation of the jacobian constant.

With a tenfold Jupiter mass ($m_J = 0.01\, m_\odot$), we obtain $C_1 = 3.1621$ and $C_2 = 3.1495$. From C_1 and C_2, we find the minimum initial distance for unstable orbits $r_1 = 3.3$ AU, and $r_2 = 3.4$ AU, respectively. In good agreement, the experiments proved configurations with an initial distance $r > 3.5$ AU to be unstable. By comparison, also orbits with a hundredfold Jupiter mass were computed. For this mass the constants are $C_1 = 3.5587$ and $C_2 = 3.4447$ and the maximum distance of unstable orbits $r_1 = 2.3$ AU and $r_2 = 2.5$ AU, while the experiments yielded $r > 2.55$ AU, again in good agreement.

It must be mentioned that in the experiments, also the inner planets Venus, Earth, and Mars were included. In this case, a zero-velocity curve is strictly speaking not defined. Accordingly, it could happen that also for $C > C_1$, the orbit of a planetoid becomes unstable because of an encounter with an inner planet. In this case the jacobian "constant" (which is no more conserved), if calculated as above, would assume a value $< C_2$ after the encounter. This never happened in the experiments (mainly because of the small eccentricities).

For planetoids with orbits close to those of Venus, Earth, or Mars, it is again sufficient to consider only the planet in question, if the orbits are not highly eccentric. The three-body problem can, as above, be treated as "restricted" with the jacobian integral C. In Eq. (3), the Jupiter mass is then to be replaced by the mass of the planet in question. In Table 1, there are given the domaines of the initial distances of planetoids (with zero initial eccentricity), which should lead to stable orbits (first column). They are determined from the condition $C = C_1$. In comparison, the experimental results of Section 5 are quoted (second column). The agreement is very good (in the small region between Venus and Earth, in which no stable orbits have been found experimentally, the three-body approximation is especially unfavourable, because the influences of Venus and Earth are almost equal).

Table 1. Stability zones of initial distances of planetoids outside the commensurabilities 1:1 (in AU)

Theoretical	Experimental
<0.63	<0.62
0.84 – 0.86	–
1.17 – 1.41	1.16 – 1.40
1.64 – 3.34	1.63 – 3.5

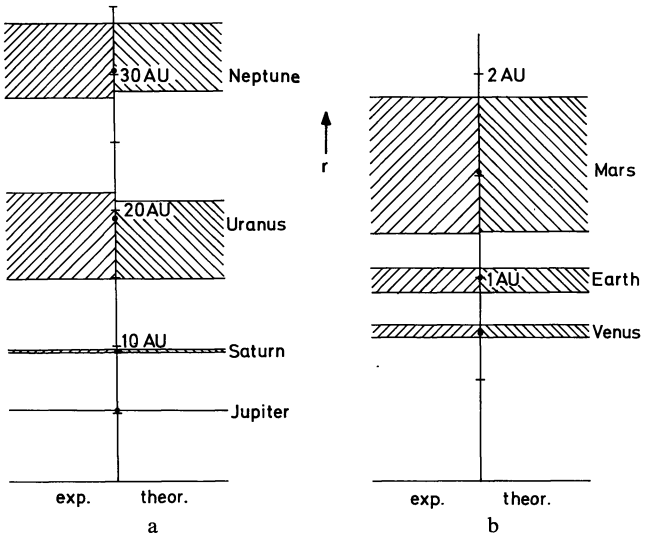

Figs. 8a and b. Experimental and theoretical stability zones of the initial distances, r (hatched areas) of the outer planets (case (a)) and the inner ones (case (b))

6.2. Planets

The jacobian integral and thus the zero-velocity curves do not exist in the three-body problem with two finite planetary masses. If the masses of the planets differ by more than one order of magnitude and if the eccentricities are sufficiently small, it is allowed to neglect the smaller mass. In this case, the stability problem can be treated as in Section 6.1.

In the case, in which the masses are almost equal, we also apply formally $C > C_1$ as stability criterion defining C by replacing in Eq. (3) the mass of Jupiter by the sum of the masses of the two planets considered. This means that we treat the problem approximately as a restricted problem in a way as if one planet had taken over the mass of the other one. The condition $C = C_1$ (or $C = C_2$, the results are almost identical) yields then again limiting distances for unstable orbits. Figures 8a and b show the stability zones calculated in this way in comparison with the experimentally found zones. The agreement is indeed very good, as well for the inner as for the outer planets.

6.3. Explicit Representation for Small Masses

The stability limits for planets and planetoids are given only implicitely by the condition $C = C_1$ (or $C = C_2$). However, for small values of $\mu (\mu = m_J/m_\odot$, or $\mu = (m_{\text{planet 1}} + m_{\text{planet 2}})/m_\odot)$ an explicit expression can be obtained from Eq. (3) by expansion in $\mu^{1/3}$. If r is the distance of the planet in question, the limits of the initial distances of unstable orbits, r_+ and r_-, are then given by

$$r_\pm = r\left(1 \pm \sqrt{12}\left(\frac{\mu}{3}\right)^{1/3}\right). \tag{5}$$

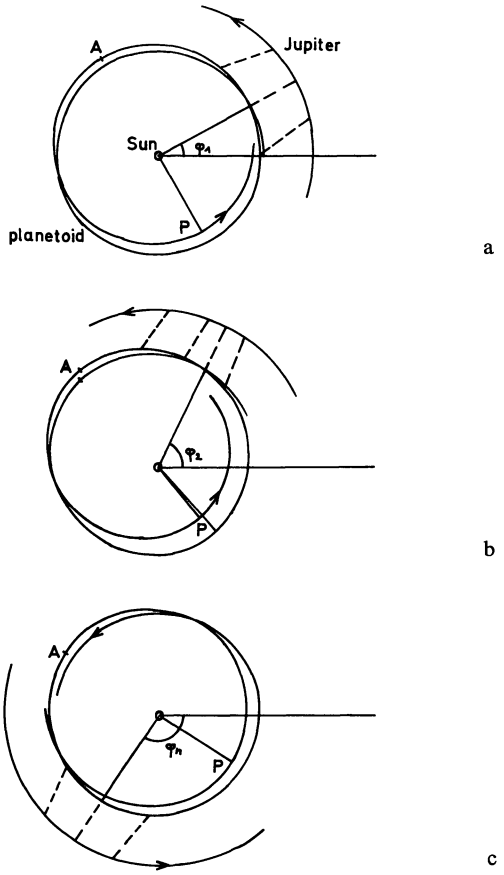

Figs. 9a–c. Parts of the orbit of a planetoid and Jupiter which are close to the commensurability 1:2, near the first (a) and the second (b) conjunction and another conjunction after some revolutions (c). Dashed lines connect points which the two bodies reach simultaneously. φ_1, φ_2, and φ_n are the phase angles of the three conjunctions. P mark the perihelion and A the aphelion of the orbit of the planetoid

Eq. (5) follows as well from the condition $C = C_1$ as from $C = C_2$ (the initial longitude is assumed to be non zero in the co-rotating system, the initial eccentricities are again taken as zero). From this, we obtain the minimum separation Δ (in units of r) of two planets on stable orbits

$$\Delta = 2.4\,\mu^{1/3},$$

and the stability criterion

$$\frac{\mu}{\Delta^3} < 0.07\,. \tag{6}$$

A similar law, $\mu/\Delta^3 = 10^{-4}$, for the separations of the planets and for the satellite systems, was found by Kuiper (1949).

7. The Role of Commensurabilities

In Section 6 we determined stability limits of the *initial* distances of the planets or the planetoids. These

limits, which agree well with those experimentally found, are determined independent of any commensurabilities. The experiments, however, have shown that the stability limits of the *mean* semi-major axes coincide with simple commensurabilities of the type $(n+1):n$. These are characterized by the fact that conjunctions occur at *one* phase angle.

We consider as a typical example the motion of a planetoid near the commensurability 1:2 with the Jupiter period (i.e. one of the experiments reported in Section 5; a similar model is described by Alfvén and Arrhenius, 1970). An alteration of the orbit is only possible by a close encounter with Jupiter, i.e. only in the neighbourhood of the conjunction.

Figure 9 shows parts of the computed orbits of the planetoid and Jupiter. Before the first encounter, the orbit of the planetoid is almost circular (Fig. 9a). The period (T_p) is slightly larger than half of the period of Jupiter (T_J). The radial component of the attraction of Jupiter bends the orbit of the planetoid slightly outward, so that in the second part of the encounter (after the conjunction), the planetoid comes nearer to the orbit of Jupiter than in the first part. Hence the deceleration due to the azimutal component of the attraction of Jupiter is slightly larger than the acceleration in the first part. The net effect is that the orbit becomes smaller and the period shorter, with an increased eccentricity. However, in the present example, T_p remains still larger than 1/2 T_J. Therefore, the phase angle of the second conjunction (φ_2) is larger than the phase angle of the first one (φ_1), and hence the conjunction occurs somewhat closer to the aphelion (Fig. 9b). This results in a stronger perturbation by Jupiter. In addition, the deceleration exceeds the acceleration more than during the first encounter, on account of the larger eccentricity, so that after the second encounter, T_p is smaller than 1/2 T_J. Therefore, the phase angle of the next encounter diminishes and moves closer to the perihelion, where the effect of an encounter becomes slighter. As long as the encounter occurs after the perihelion passage, the deceleration is always larger than the acceleration. The period therefore diminishes further, and the eccentricity increases though only to a smaller extent. When the phase angle grows smaller than the perihelion angle, the behavior reverses. The planetoid is accelerated at every encounter and the period increases again. Simultaneously the eccentricity decreases until the orbit becomes again almost circular (Fig. 9c) and the initial state is practically restored. Then the behavior starts anew as described above, however with a new perihelion angle. So the conjunction moves through the aphelion of the orbit of the planetoid while the eccentricity practically vanishes. Hereby the conjunction in average moves retrograde, i.e. the period happens to be somewhat smaller than 1/2 T_J (this is in contrast to highly eccentric orbits as described by Alfvén and Arrhenius, 1970).

Qualitatively the same behavior as described above for a planetoid is found for two planets with comparable masses. Here both orbits change during an encounter in opposite directions. When the inner planet is decelerated and its period T_i accordingly diminished, the outer one is accelerated and its period T_a increased. Both effects tend to increase the ratio T_a/T_i.

The above described behavior holds for the other commensurabilities of the type $(n+1):n$, too. Which commensurability actually is responsible for the stability limit, depends on the magnitude of the perturbation forces, i.e. on the masses of the planets concerned and on the minimum possible separation, which depends on the orbital eccentricities. The limiting commensurability can be inferred from the results of Section 6. That commensurability of the type $(n+1):n$, which is closest to the calculated limit inside or possibly slightly outside the stability zone, should be responsible for the limits of the long time averages of the semi-major axes of stable systems. These considerations indeed lead to the observed limiting commensurabilities 2:1, 3:2 (case (a)) and 4:3, 5:4 (case (b)).

8. The Role of the Masses

In the experiments, described in Section 4 and 5, we adopted increased planetary masses in order to reduce the computing time. Now we have to check, how much the planetary masses affect the stability zones. For this reason, a number of experiments was carried out for 1, 2, 5, and 10-fold masses in the case of the outer planets and the stability limits determined (Fig. 10, arrows). Furthermore, the stability limits were calculated by means of the jacobian constant (as in Section 6) and plotted in Fig. 10 for comparison (fully drawn lines). They agree well, especially for small masses, as is to be expected. The critical commensurabilities vary in steps, indicated by the numbers in Fig. 10. As one can see, the width of the stability zones increases by roughly a factor of 1.7 when the masses are reduced to the present values. The bands narrow to nearly the present distances when the masses are increased by roughly a factor of 100, as we can infer from extrapolation. The centers of the stability zones remain almost constant when the masses are varied.

9. Discussion

The experiments yielded stability zones for the semi-major axes of the planetary orbits which are separated by gaps, in which no stable orbits are possible (Fig. 3). The present semi-major axes lie in the middle of these zones. Though the runs cover only a few thousand years, it is reasoned that the results are independent of the length of the experiments. The arguments are based

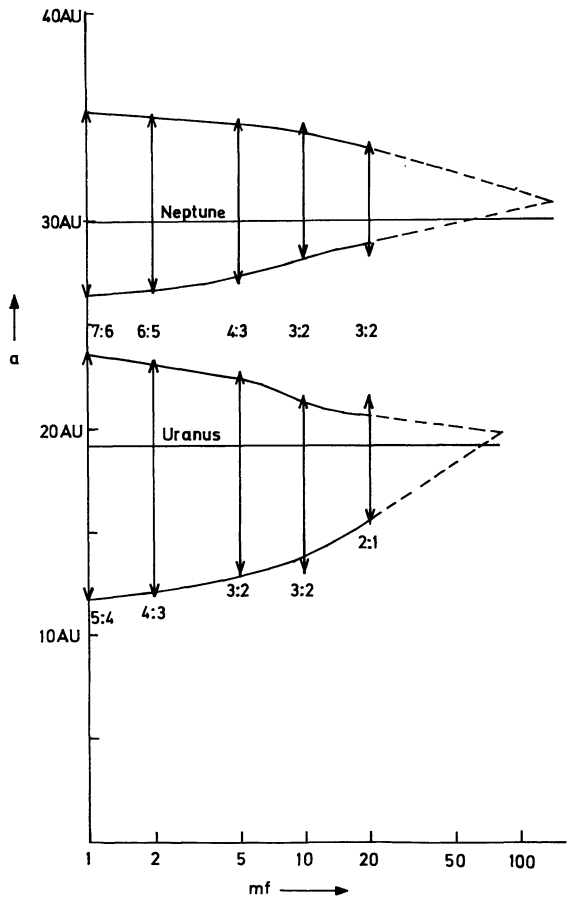

Fig. 10. Stability limits of the semi-major axes of the major planets Neptune and Uranus as a function of the mass factor, mf (adopted mass/present mass). Full lines: calculated limits; double arrows: experimentally found limits. The corresponding limiting commensurabilities are quoted. Dashed lines indicate extrapolated limits. The straight lines mark the present distances

on the discussion of the zero-velocity curves and the role of commensurabilities in Section 6 and 7.

It is highly improbable that the present planets have been formed outside the stability zones. For, if the planetary system started with the present planets and with some of their orbits falling into the instability gaps, then the system would have become unstable within a short time, with the effect that at least one planet would have been ejected. If the system started with more than nine planets and the present planets were forced into the stability zones by two-body encounters with the additional planets (which resulted in a subsequent ejection of these planets), high eccentricities should be more frequent than is observed in the present system.

The width of the stability zones depends on the assumed masses. For about 100-times increased masses of the major planets, practically only the present semi-major axes are allowed. If the proto-planets started with such masses (Kuiper, 1951), the present configuration was enforced only by gravitational interaction. If on the other hand the primeval masses of the planets never exceeded the present values, some additional agents have influenced the present configuration. Probably the most important agent is viscosity at an early stage of planetary formation. Preliminary experiments (not presented here) have shown that in this case, an initial unstable orbit is forced into a stable zone while the eccentricity goes to zero.

Acknowledgements. It is a pleasure to thank Professor K. Hunger for suggesting the problem, for many helpful discussions, and for critical reading of the manuscript.
The calculations have been carried out with the CDC 6500 of the Technische Universität Berlin.

References

Alfvén, H., Arrhenius, G. 1970, *Astrophys. Space Sci.* **8**, 338.
Giacaglia, G.E.O. (Editor) 1970, Periodic Orbits, Stability and Resonances. Reidel Publishing Comp., Dordrecht-Holland.
Hagihara, Y. 1961, The stability of the solar system, in *Planets and Satellites*, Ed. G. P. Kuiper, B. M. Middlehurst, Univ. Chicago Press, Chicago.
Hills, J.G. 1970, *Nature* **225**, 840.
v. Hoerner, S. 1960, *Z. Astrophys.* **50**, 184.
v. Hoerner, S. 1963, *Z. Astrophys.* **57**, 47.
Kristensen, L.K. 1970, A Program for Numerical Integration of the Classical Many-body Problem in Elements, private communication.
Kuiper, G.P. 1949, *Astrophys. J.* **109**, 308.
Kuiper, G.P. 1951, On the origin of the solar system, in *Astrophysics*, Ed. J. A. Hynek, McGraw-Hill, New York-Toronto-London.
Kumar, S.S. 1971, *Nature* **233**, 473.
Mikhlin, S.G., Smolitskiy, K.L. 1967, Approximate Methods for Solution of Differential and Integral Equations (translated from the Russian), American Elsevier Publishing Comp., New York.
Ovenden, M.W. 1972, *Nature* **239**, 508.
Shelus, P.J., Kumar, S.S. 1970, *Astron. J.* **75**, 315.
Stumpff, K. 1965, Himmelsmechanik, Band. II. VEB Deutscher Verlag der Wissenschaften, Berlin.
Szebehely, V. 1967, Theory of Orbits. Academic Press, New York-London.
ter Haar, D., Cameron, A.G.W. 1963, in *Origin of the Solar System*, Academic Press, New York-London.
v. Weizsäcker, C.F. 1943, *Z. Astrophys.* **22**, 319.
Williams, J.G., Benson, G.S. 1971, *Astron. J.* **76**, 167.

J. Birn
Institut für Astrophysik
Technische Universität Berlin
D-1000 Berlin 10
Ernst-Reuter-Platz 7
Germany